Talanta 83 (2011) 1134–1146

Contents lists available at ScienceDirect

Talanta

journal homepage: www.elsevier.com/locate/talanta

Comprehensive description of the photodegradation of bromophenols using chromatographic monitoring and chemometric tools

Sílvia Mas[a,b,*], Albert Carbó[a], Sílvia Lacorte[b], Anna de Juan[a], Romà Tauler[b]

[a] Chemometrics Group, Department of Analytical Chemistry, Universitat de Barcelona, Av. Diagonal, 647, 08028 Barcelona, Catalonia, Spain
[b] Environmental Chemometrics Group, Department of Environmental Chemistry, Institute of Environmental Assessment and Water Diagnostic (IDAEA-CSIC), Jordi Girona 18, Barcelona, 08034 Barcelona, Catalonia, Spain

ARTICLE INFO

Article history:
Available online 1 August 2010

Keywords:
Bromophenols
Photodegradation process
Chromatographic monitoring
Multivariate curve resolution-alternating least squares (MCR-ALS)
Soft-modeling
Process analysis

ABSTRACT

A general procedure for the study of complex photodegradation processes of environmental pollutants based on chromatographic monitoring and chemometric method is proposed. The procedure consists of multiset data analysis of aliquots collected at different reaction times and injected in High-Performance Liquid Chromatography coupled to diode array detection and mass spectrometry (HPLC–DAD-MS). In this study, photodegradation of six bromophenols with different degrees of bromination has been investigated in order to find out their photodegradation pathways and kinetics and to show the potential of the procedure proposed. Multivariate curve resolution-alternating least squares (MCR-ALS) has been used to resolve chromatographic elution profiles and pure spectra of species involved in the photodegradation process and, hence, to elucidate the photodegradation mechanism and to propose the chemical structure of the main photoproducts. This study shows that chromatographic monitoring is the preferred option when photochemical systems with large number of components with similar spectra and kinetic evolution are analyzed. This work reveals the advantages of the double DAD and MS detection to provide mechanistic and structural information about these complex photodegradation processes.

1. Introduction

Flame retardants are used to prevent accidental fires by reducing the flammability of combustible materials such as plastics and synthetic polymers. The most important group of flame retardants is the brominated flame retardants (BFRs), which contain a diversity of chemicals such as polybrominated biphenyls (PBBs), tetrabromobisphenol A (TBBPA), polybrominated diphenyl ethers (PBDEs), hexabromocyclododecane (HBCD) and bromophenols (BP).

Due to the observed increase of these compounds in the environment and in humans and to the proven toxicity of lowly brominated congeners, often banned by environmental policies, concerns about the risk of all BFR compounds have arisen [1]. Assuming that the now in use highly brominated congeners seem to degrade into lowly brominated congeners by the action of light, it is relevant to understand the photodegradation process of BFRs compounds to better understand their environmental fate.

Several studies have proven that BFRs can be degraded by ultraviolet (UV) light and direct sunlight under a variety of conditions [2–24]. Extensive data exists on the identity of transformation products of, e.g., PBDEs [2–16], TBBPA [17], and rates of degradation have been reported for these compounds [6,8–9,11,12,17].

Bromophenols comprise 19 congeners from mono- to pentabrominated compounds, with physicochemical properties, such as solubility, volatility, and octanol–water partition coefficient (Kow), varying systematically as a function of the degree of bromination and the substitution pattern. The position and number of bromine atoms on the benzene ring may also play a relevant role in the photodegradation rates and mechanism, as it has been observed in the photodegradation studies of their homologs, the chlorophenols [18–20]. Photodegradation of monobromophenols has been investigated in previous works, but the studies are mainly focused on the identification of the photodegradation products without entering in depth into the degradation pathways involved [20–26]. The scarcity of works about polybrominated compounds is even larger and to the knowledge of the authors, no detailed mechanistic photochemical works have been conducted on these highly brominated compounds. Obtaining this information and providing the necessary methodology for this purpose and, in general, for monitoring and interpretation of complex photodegradation processes is the main goal of the present work.

We have recently studied the photodegradation processes of decabromodiphenyl ether (a PBDE compound) [27] and of nitro-

* Corresponding author at: Chemometrics Group, Department of Analytical Chemistry, Universitat de Barcelona, Av. Diagonal, 647, 08028 Barcelona, Catalonia, Spain. Tel.: +34 93 403 44 45; fax: +34 93 402 12 33.
E-mail address: silviamas@ub.edu (S. Mas).

0039-9140/$ – see front matter © 2010 Elsevier B.V. All rights reserved.
doi:10.1016/j.talanta.2010.06.042

furazone (a well-known antibacterial agent) [28] under UV light by classical UV–visible (UV–vis)-spectrophotometric monitoring, i.e., collecting spectra from the solution of the compound of interest as a function of time, followed by the application of chemometric tools. For this kind of experiments, the hybrid hard- and soft-modeling multivariate curve resolution-alternating least squares (HS-MCR) [29] provided an efficient methodology for the comprehensive study of this kind of processes, helping in the interpretation of the degradation steps. HS-MCR provided kinetic profiles and pure spectra of the photodegradation products and the rate constants of the process. However, in both studies, the presence of identical (or very similar) kinetic and spectra profiles among the species involved in the photodegradation process made that the components resolved by HS-MCR had to be interpreted as mixtures of congeners (or compounds of similar behavior) rather than as single specific chemical compounds. Preliminary soft-modeling MCR [30–33] resolution results on few chromatographic data (model-free experiments) for the same systems confirmed the complexity of the degradation processes, since the number of compounds modeled from the chromatographic runs was higher than the number of species resolved in the classical spectroscopic experiments. Indeed, the different elution behavior of these compounds is the reason why they can be individually modeled, even though they may present an identical kinetic evolution or very similar spectra. Therefore, analysis of chromatographic data is the preferred option when photodegradation processes from systems with large number of compounds or with compounds with similar spectra and kinetic evolution must be analyzed, as it has also been seen in previous works [34–36].

In the present work, the photodegradation of six bromophenol congeners with different degrees of bromination has been investigated. Assuming the complexity of the photodegradation processes, instead of using the classical spectroscopic monitoring, where reactions are followed by spectroscopic method and interpreted by HS-MCR, the photodegradation processes have been monitored by high performance liquid chromatography coupled to diode array detection and to mass spectrometry (HPLC–DAD-MS) and interpreted by multiset analysis by MCR-ALS. Aliquots collected at different reaction times have been injected and analyzed simultaneously in order to resolve chromatographic elution profiles and pure spectra of the photodegradation products, to propose the chemical structure of the main photoproducts and to elucidate the mechanism of the degradation process. The double DAD and MS detection provides clear advantages. On one hand, the high signal/noise ration in DAD detection is better at discriminating all eluted compounds among them and, hence, to provide a global picture of their kinetic evolution. On the other hand, MS detection provides resolved MS spectra with easily interpretable features useful for compound identification.

2. Experimental

2.1. Chemicals

2-Bromophenol (2BP), 3-bromophenol (3BP), 4-bromophenol (4BP), 2,4-dibromophenol (24DBP), 2,4,6-tribromophenol (246TBP) and 2,3,4,5,6-pentabromophenol (PBP) (98–99% purity) were purchased from Sigma–Aldrich Corp. (St. Louis, MO USA) and used without further purification.

Ammonium acetate and acetic acid (analytical grade) and acetonitrile and methanol (HPLC-grade) were supplied by Merck (Darmstadt, Germany). Finally, MilliQ water, with a conductivity <0.05 $\mu S\,cm^{-1}$, was obtained using a MilliQ water purification system (Millipore, Mosheim, France).

2.2. Apparatus and experimental setup

2.2.1. Photodegradation setup

The photodegradation of bromophenols was carried out in a cylindrical annular batch reactor equipped with a UV lamp. The reactor consisted of an immersion quartz tube (2.5 cm i.d., and 38 cm in length), which held a low-pressure mercury vapor lamp (LPML) of 15 W (Heraeus Noblelight, Germany). The light source emitted predominantly at 254 nm. The quartz tube was placed in a Pyrex glass outer reactor (with a capacity of 0.7 l).

2.2.2. Chromatographic setup

Chromatographic equipment consisted of a Waters 2690 series Alliance HPLC (Waters, Milford, MA), with a quaternary pump equipped with a 120 vial capacity sample management system. The liquid chromatograph was coupled to a Waters 9960 diode-array (DAD) and mass spectrometer (MS) detection systems in tandem.

The analytes were separated on a 250 mm × 4 mm, I.D. 5 μm C_{18} reversed phase column LiChrospher 100 RP-18 column (Merck). The sample injection volume was set at 30 μL. A ternary isocratic mobile phase with 55% methanol/acetonitrile (25:75) and 45% acetic acid/acetate buffer pH 3.5 (B) was used at a flow rate of 1000 μL/min. An Orion 510 pH-meter was used to verify the suitable pH of the mobile phase.

Within the DAD-MS detection system, MS detection was carried out on a benchtop triple quadrupole mass spectrometer Quattro LC from Micromass (Manchester, UK) with APCI (atmospheric pressure chemical ionization) interface at the following conditions: capillary voltage −3.0 kV, cone voltage −30 V, source and desolvation temperatures 150 and 500 °C, respectively, nitrogen (99.999% purity) flow 48 L/h for the cone gas and 325 L/h for desolvation gas. The MS detector was operated in scan mode (70–600 amu) with scan duration of 1 s/scan and an interscan time of 0.1 s. The DAD detection in the UV–vis range was operated at spectral resolution of 1.2 nm in the spectral range from 200 to 500 nm and collecting one spectrum per second.

2.3. Experimental procedure

The bromophenol solutions were prepared in mobile phase at a concentration of ca. 7×10^{-4} M. The samples were placed in the photoreactor and were irradiated by the low-pressure mercury vapor lamp a room temperature. At different time intervals selected during the photodegradation process, aliquots of 1 mL of the sample were collected and analyzed by HPLC–DAD-MS. Table 1 shows the different process times at which aliquots from bromophenol solution were collected for later injection. Time intervals were selected based on simple auxiliary studies done only with classical spectroscopic monitoring on the same kind of compounds, where it was seen a faster spectroscopic evolution at the beginning of the process. This is the reason why the time intervals among the first aliquots collected are smaller than the ones at the end.

3. Data analysis

3.1. Data acquisition

Masslynx (version 3.5) was the software supplied with the mass spectrometer of Micromass (Manchester, UK) for control, data acquisition and data preprocessing. DataBridge was a file converter provided with Masslynx to convert LC–DAD-MS raw files into an ASCII format. Matlab® for Windows (version 7.0) was used for data preprocessing, programming, calculations and graphical representation. An in-house written Matlab routine was employed to convert the ASCII format into Matlab readable files. Following this procedure, the data obtained from each LC–DAD-MS raw file were

Table 1
Process times at which aliquots from each bromophenol solution were collected for later injection in HPLC–DAD-MS.

Aliquot number	Process time (min)					
	2BP	3BP	4BP	24DBP	246TBP	PBP
1	0	0	0	0	0	0
2	1	1	1	1	2	1
3	2	2	2	3	5	5
4	3	4	3	5	8	8
5	4	5	4	7	10	10
6	5	7	10	10	15	15
7	10	10	15	21	24	20
8	15	15	20	30	32	30
9	20	20	30	40	40	40
10	45	30	40	50	70	65
11	54	40	50	65	90	91
12	63	50	60	105	120	120
13	90	65	80	145	136	160
14	102	81	100	180	152	200
15	120	100	120	225	227	230
16	168	122	150	295	302	320
17	180	150	180	364	360	386
18	210	189	210	433	390	416
19	238	210	240	480	421	446
20	300	240	300			
21	390	324	360			
22		360	390			
23		420				

finally organized into two data matrices: one for the chromatogram with DAD detection and another one for the chromatogram with MS detection.

3.2. Data structure

Each chromatographic run coming from an aliquot of a particular k process time provided two data matrices: one for DAD detection, $\mathbf{D}_{k(DAD)}$ and another one for MS detection, $\mathbf{D}_{k(MS)}$, which can be described by the bilinear model in Eq. (1).

$$\mathbf{D}_{k(\text{DAD or MS})} = \mathbf{C}_{k(\text{DAD or MS})}\,\mathbf{S}^{T}_{k(\text{DAD or MS})} + \mathbf{E}_{k(\text{DAD or MS})} \quad (1)$$

Rows of matrices $\mathbf{D}_{k(DAD)}$ and $\mathbf{D}_{k(MS)}$ are the UV–vis or MS spectra recorded at different elution times, and columns of matrices $\mathbf{D}_{k(DAD)}$ and $\mathbf{D}_{k(MS)}$ are the chromatographic elution profiles recorded at different wavelengths and at different m/z, respectively. $\mathbf{C}_{k(DAD)}$ and $\mathbf{C}_{k(MS)}$ are the matrices of the elution profiles of the resolved pure compounds during a particular chromatographic run in the analysis of aliquot (process time) k by means of DAD and MS detection, respectively. $\mathbf{S}^{T}_{k(DAD)}$ and $\mathbf{S}^{T}_{k(MS)}$ are the matrices of the related resolved pure spectra. Finally, $\mathbf{E}_{k(DAD)}$ and $\mathbf{E}_{k(MS)}$ are the noise contributions not included in the bilinear model (see Fig. 1a).

The same bilinear model holds for the multiset structures formed by all the chromatographic runs coming from the aliquots collected at the different N times of the photodegradation process

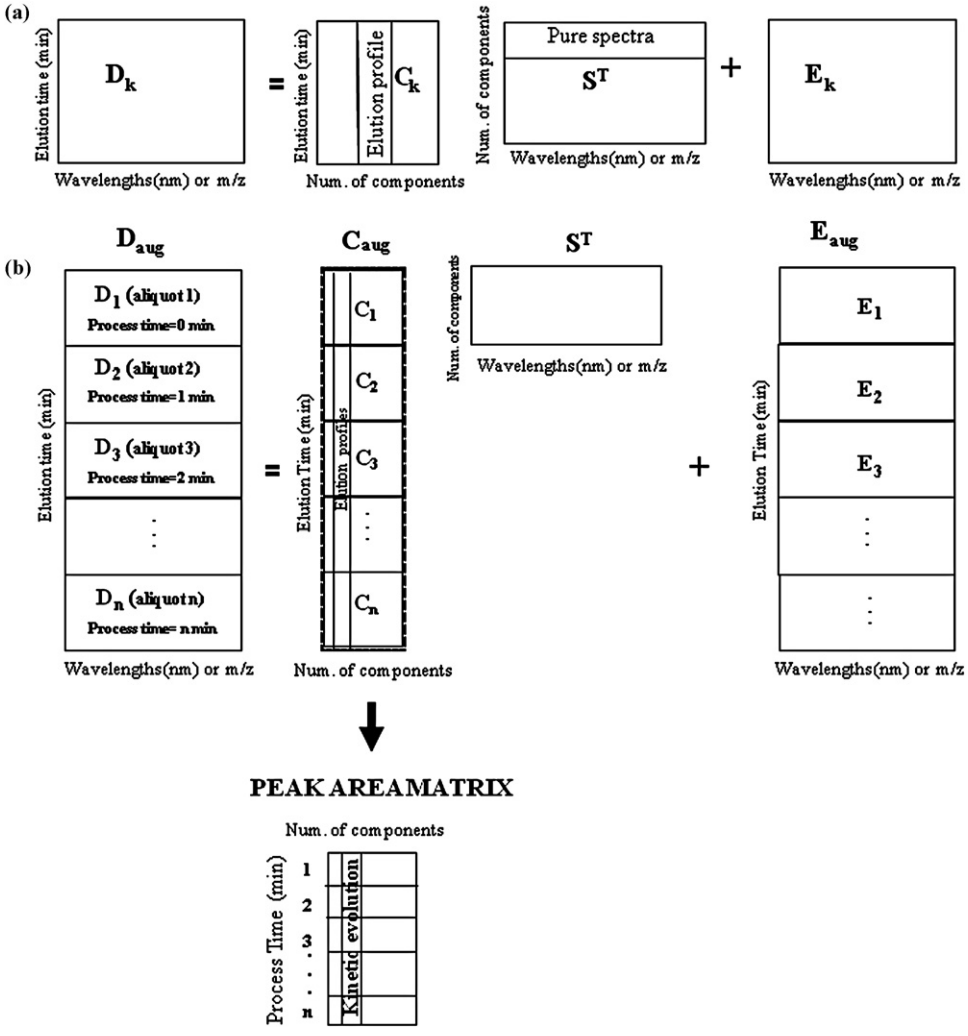

Fig. 1. (a) Multivariate curve resolution-alternating least squares (MCR-ALS) applied to the single data matrix $\mathbf{D}_{k(\text{DAD or MS})}$ and (b) MCR-ALS applied to the column-wise augmented data matrix $\mathbf{D}_{aug(\text{DAD or MS})}$. $\mathbf{D}_1$, $\mathbf{D}_2$, $\mathbf{D}_3$ and $\mathbf{D}_n$ are the aliquots collected at the different process times.

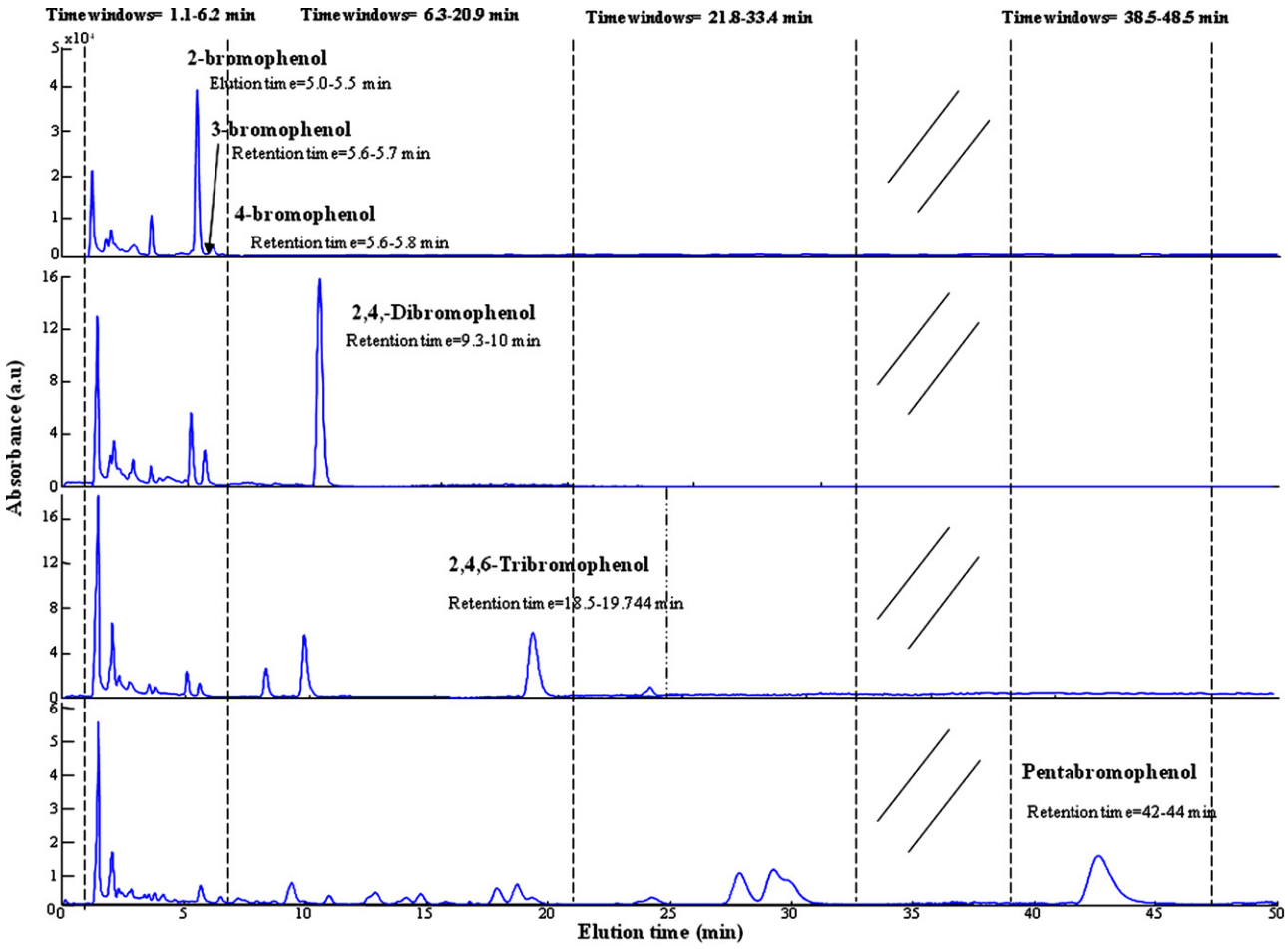

Fig. 2. Time window design applied to the chromatograms of monobromophenols, 2,4-dibromophenol, 2,4,6-tribromophenol and pentabromophenol. The picture shows the mean chromatograms of these compounds at an intermediate process time. The retention time of the parental compound is identified. Dashed lines delimit time window boundaries.

($k = 1, 2, \ldots, N$). These multiset structures are organized by setting the data matrices $\mathbf{D}_{\mathbf{k(DAD\ or\ MS)}}$ one on top of each other (column data matrix augmentation). The new column-wise augmented data matrix $\mathbf{D}_{\mathbf{aug(DAD\ or\ MS)}}$ (see Fig. 1b) obeys now the extended bilinear model equation.

$$\begin{aligned}\mathbf{D}_{\mathbf{aug(DAD\ or\ MS)}} &= [\mathbf{D}_{\mathbf{1(DAD\ or\ MS)}};\ \mathbf{D}_{\mathbf{2(DAD\ or\ MS)}};\ \ldots;\ \mathbf{D}_{\mathbf{N(DAD\ or\ MS)}}] \\ &= [\mathbf{C}_{\mathbf{1(DAD\ or\ MS)}};\ \mathbf{C}_{\mathbf{2(DAD\ or\ MS)}};\ \ldots;\ \mathbf{C}_{\mathbf{N(DAD\ or\ MS)}}] \\ &\quad \mathbf{S}^{\mathbf{T}}_{\mathbf{(DAD\ or\ MS)}} + [\mathbf{E}_{\mathbf{1(DAD\ or\ MS)}};\ \mathbf{E}_{\mathbf{2(DAD\ or\ MS)}};\ \ldots; \\ &\quad \mathbf{E}_{\mathbf{N(DAD\ or\ MS)}}] = \mathbf{C}_{\mathbf{aug(DAD\ or\ MS)}}\mathbf{S}^{\mathbf{T}}_{\mathbf{(DAD\ or\ MS)}} \\ &\quad + \mathbf{E}_{\mathbf{aug(DAD\ or\ MS)}} \qquad (2)\end{aligned}$$

where $\mathbf{C}_{\mathbf{aug(DAD\ or\ MS)}}$ is a column-wise augmented matrix formed by the $\mathbf{C}_{\mathbf{k(DAD\ or\ MS)}}$ submatrices that contain the resolved elution profiles in the different chromatographic runs, and $\mathbf{S}^{\mathbf{T}}_{\mathbf{(DAD\ or\ MS)}}$ is (as in Eq. (1)), the single matrix of pure spectra of the resolved compounds, common to all chromatograms analyzed. $\mathbf{E}_{\mathbf{aug(DAD\ or\ MS)}}$ contains the noise not included in the bilinear model.

From the bilinear model of several chromatographic runs related to the aliquots collected at different times of the photodegradation process, kinetic profiles of the compounds involved in the photodegradation process can also be derived by displaying the evolution of the areas of the resolved peaks as a function of the process time (see Fig. 1b).

3.3. Data pretreatment

Before recovering the bilinear model expressed in Eq. (2) from the raw data by multivariate curve resolution (see Section 3.4), some data pretreatments were applied to solve problems related to the data matrix size and to the large number of compounds to be resolved.

Photodegradation experiments monitored by series of chromatograms that present many chromatographic peaks hinder the complete resolution of the data set, particularly when the pure spectra of the different compounds are similar among them. In order to facilitate a good differentiation among the compounds involved in the photodegradation process, elution time-windowing [37,38] was carried out taking into account the number of compounds of the chromatograms and the elution windows of families of compounds of interest. Fig. 2 shows the boundaries of the time windows set for the different bromophenols studied, taking as a reference for visualization the mean chromatogram of one of the aliquots injected during the degradation process. Looking at the retention times of the parental bromophenols, it can be seen that time windows often separate compounds with different degrees of bromination. In all cases, time windows were easy to set because clear peak clusters could be distinguished in the chromatographic runs.

Once the time windows for each photodegradation process were set, one or several multiset structures built with analogous time windows from the different chromatographic runs were

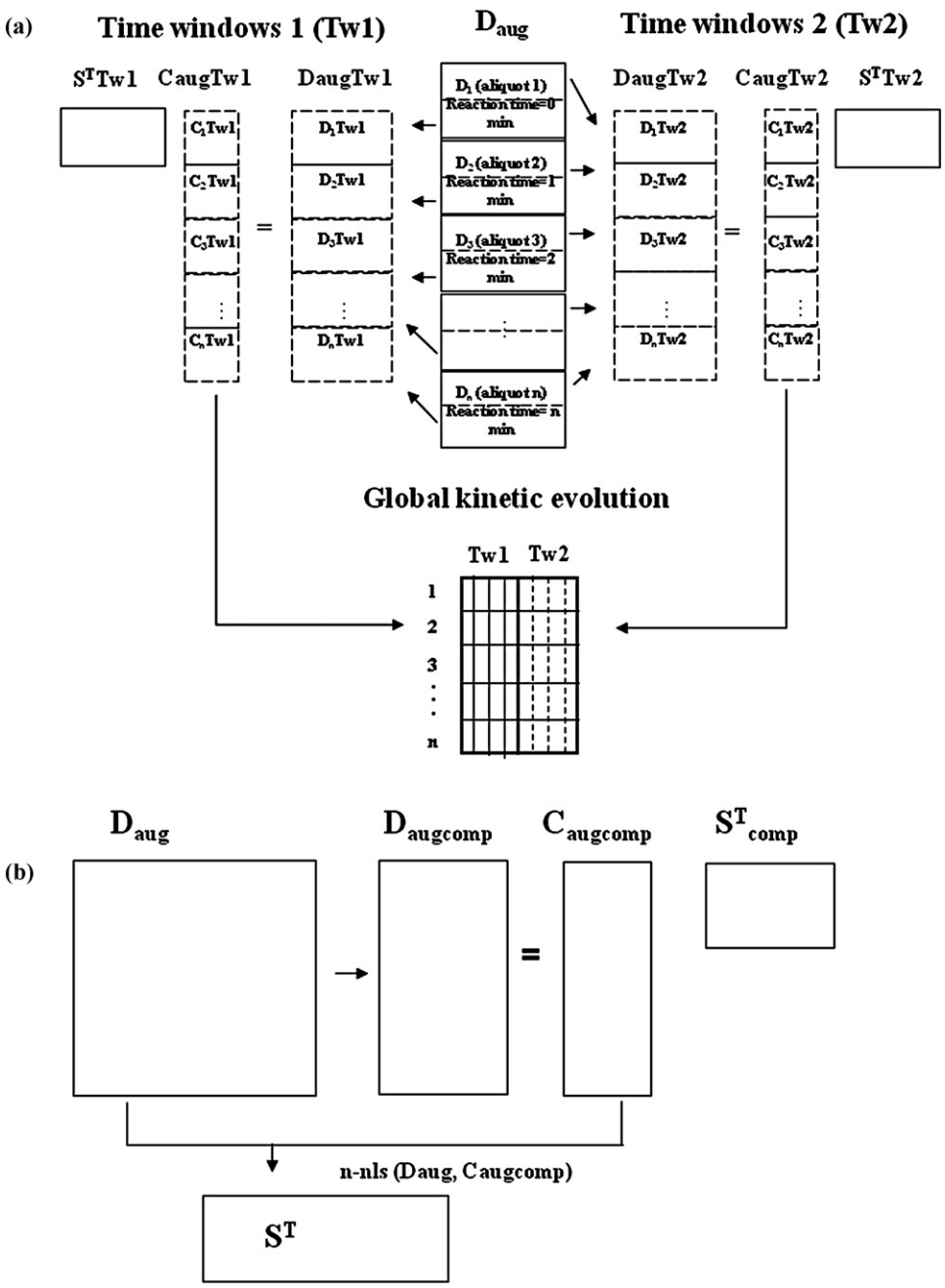

Fig. 3. (a) Time windowing strategy applied to the resolution column-wise augmented data matrix $\mathbf{D_{aug(DAD\ or\ MS)}}$, $\mathbf{C_i tw_j}$ and $\mathbf{St_i w_j}$ refer to resolved elution profiles and pure spectra of each time window multiset structure, respectively. Global kinetic evolution is obtained by appending peak areas of resolved compounds from both time window multiset structures (b) MCR-ALS applied to compressed data matrix $\mathbf{D_{augcomp(MS)}}$ and non-negative least squares (n-nnls) recuperation of the full resolved spectra.

analyzed independently. The global interpretation of the kinetic evolution of compounds involved in the photodegradation process can be obtained by considering altogether the results of all multiset structures derived from the same photodegradation process (see Fig. 3a).

Due to the relative large size of MS spectra (580 m/z values for each individual MS spectrum), compression of $\mathbf{D_{aug(MS)}}$ in the spectral direction was done by suppressing m/z channels with irrelevant information. The mean mass spectrum of $\mathbf{D_{aug(MS)}}$ was taken as the reference to perform the elimination of irrelevant m/z channels and the m/z channels showing less than 1% of intensity with respect to the maximum were removed. Such a procedure provided a compression from 580 to 90–180 m/z channels in each MS spectrum. A new compressed data matrix $\mathbf{D_{augcomp(MS)}}$ keeping the relevant chemical information present in the original data matrix $\mathbf{D_{aug(MS)}}$ was obtained. The new compressed data matrix $\mathbf{D_{augcomp(MS)}}$, obeys also the bilinear model:

$$\mathbf{D_{augcomp(MS)}} = \mathbf{C_{augcomp(MS)}}\mathbf{S^T_{comp(MS)}} + \mathbf{E_{aug(MS)}} \quad (3)$$

where the rows of matrix $\mathbf{D_{augcomp(MS)}}$ are the compressed MS spectra. $\mathbf{C_{aug(MS)}}$ is the column-wise augmented matrix of the resolved chromatographic elution profiles, which is the final result sought since relevant information is kept in the compressed original matrix $\mathbf{D_{augcomp(MS)}}$, and $\mathbf{S^T_{comp(MS)}}$ is the matrix of their corresponding pure compressed MS spectra (see Fig. 3b). To recover the matrix of full resolved spectra, a single non-negative least squares step is

Table 2
Number of resolved components and variance explained by MCR-ALS analysis of the photodegradation experiments of the investigated bromophenols.

Bromophenols	DAD		MS	
	N. of components	r^2	N. of components	r^2
2BP	9	98.6	6	70.4
3BP	7	96.5	6	72.6
4BP	7	97.8	6	79.8
24DBP				
1.1– 6.2 min	10	96.1	6[a] (8)	57.9[b] (95.8)
6.3–12 min	2	99.9	1	94.1
246TBP				
1.1–6.2 min	9	97.5	7[a] (9)	53.3[b] (96.7)
6.3–22.0 min	6	99.9	4[a] (5)	75.6[b] (98.8)
PBP				
1.1–6.2 min	11	96.7	7[a] (9)	64.5[b] (98.7)
6.3–20.9 min	15	97.7	7[a] (8)	69.8[b] (90.8)
21.8–33.4 min	6	97.8	4[a] (3)	66.2[b] (95.8)
38.5–48.5 min	2	99.9	1	92.2

[a] Number of chemical compounds without the contribution of the background (in parenthesis, total number of components in the analysis: chemical compounds + background contribution).
[b] Explained variance by all chemical compounds without the contribution of the background (in parenthesis, explained variance by all components: chemical compounds + background contributions).

performed by doing:

$$\mathbf{S}^{T} = \mathbf{C}_{\mathbf{augcomp(MS)}}{}^{+}\mathbf{D}_{\mathbf{aug(MS)}} \quad (4)$$

where $\mathbf{C}_{\mathbf{augcomp(MS)}}{}^{+}$ is the pseudoinverse of $\mathbf{C}_{\mathbf{augcomp(MS)}}$ and $\mathbf{D}_{\mathbf{aug(MS)}}$ is the original uncompressed MS matrix.

3.4. Data treatment

Multivariate curve resolution (MCR) aims at resolving the bilinear model $\mathbf{D} = \mathbf{CS}^{\mathbf{T}}$ (shown in Eqs. (2) and (3)) by using the sole information contained in the raw data set **D** [30–33]. For this purpose, an alternating least squares (ALS) algorithm is used to refine iteratively the **C** and $\mathbf{S}^{\mathbf{T}}$ matrices so that an optimal reproduction of the experimental matrix **D** is achieved. At each iterative cycle of the optimization, matrices **C** and $\mathbf{S}^{\mathbf{T}}$ are calculated under constraints trying to minimize the reproduction error, $||\mathbf{D}\text{-}\mathbf{CS}^{\mathbf{T}}||$. The percentage of explained variance is calculated according to the expression:

$$r^2(\%) = 100 \times \frac{\sum_{ij} d_{ij}^{2*}}{\sum_{ij} d_{ij}^{2}} \quad (5)$$

where d_{ij}^{*} are the values of the data set reproduced by the bilinear model and d_{ij} the original values in the raw data set **D**.

The detailed steps of the algorithm have been described elsewhere [30–33,36,39].

In the context of the photodegradation experiments, different constraints are applied to give chemical meaning to the solutions obtained by MCR-ALS [30]. The constraints selected for the chromatographic data from the photodegradation experiments were: non-negativity (both elution profiles and pure spectra of the resolved components must be positive), normalized pure spectra and unimodality (presence of only one maximum per profile). The unimodality constraint is applied independently to each concentration submatrix in multiset structures. In our example, unimodality was applied in the DAD multiset structures to all the elution profiles in submatrices of $\mathbf{C}_{\mathbf{aug}}$, i.e., to all resolved components in the analysis of DAD data, since all elution profiles are related to a distinct pure spectrum. However, in the analysis of MS data, unimodality was not applied to all the resolved components, since compounds with identical pure MS spectra, e.g., homolog compounds, show a single pure spectrum and a related elution profile with several peaks, one per each of the retention times of the homologs within the same class. A relevant constraint in evolving systems, such as chromatographic elutions, is the use of selectivity and local rank information (some components are forced to be absent in some elution ranges). Strict selectivity, understood as the presence of a single compound in a certain elution range, was only applied at the aliquot related to process time = 0, where only the parent compound is allowed to be present. In multiset structures, the local rank information has been set taking advantage of the fact that elution patterns among chromatographic runs should be comparable since all injections were done in the same conditions. Elution windows are very clear in aliquots where the compounds are major. Therefore, in some few aliquots, and only when some compounds are really minor, it has been prevented that these minor compounds appear in an elution range very far from the one found in the runs where these compounds are dominant. In these cases, for a particular compound, a zero-component window in further elution ranges has been set as a constraint.

In the case of the compressed data matrix $\mathbf{D}_{\mathbf{augcomp(MS)}}$, once $\mathbf{C}_{\mathbf{augcomp(MS)}}$ has been estimated by ALS, application of one additional non-negative least squares step to the original non-compressed data matrix $\mathbf{D}_{\mathbf{augcomp(MS)}}$ allowed the recovery of the full non-compressed MS spectra of bromophenols and photoproducts ($\mathbf{S}^{\mathbf{T}}_{\mathbf{comp(MS)}}$), to facilitate the identification of these compounds.

Finally, the kinetic profiles of the compounds involved in the photodegradation process have been derived displaying the evolution of the areas of the resolved peaks in each chromatographic run of the multiset structures as a function of the process time in which the injected aliquots were collected (see Fig. 3a).

4. Results and discussion

As a general summary, Table 2 lists the number of resolved components and the explained variance obtained from the MCR-ALS analyses of the photodegradation experiments of each bromophenol congener. This table comprises the results achieved from both DAD and MS data resolutions with the related time windows, when necessary.

The high number of components modeled (7–9 for monobromophenols, 12 for the dibromophenol, 15 for the tribromophenol and 34 for pentabromophenol for DAD data) confirms the complexity of the photodegradation process, which prevents the complete modeling of all compounds in the bromophenol photodegradations

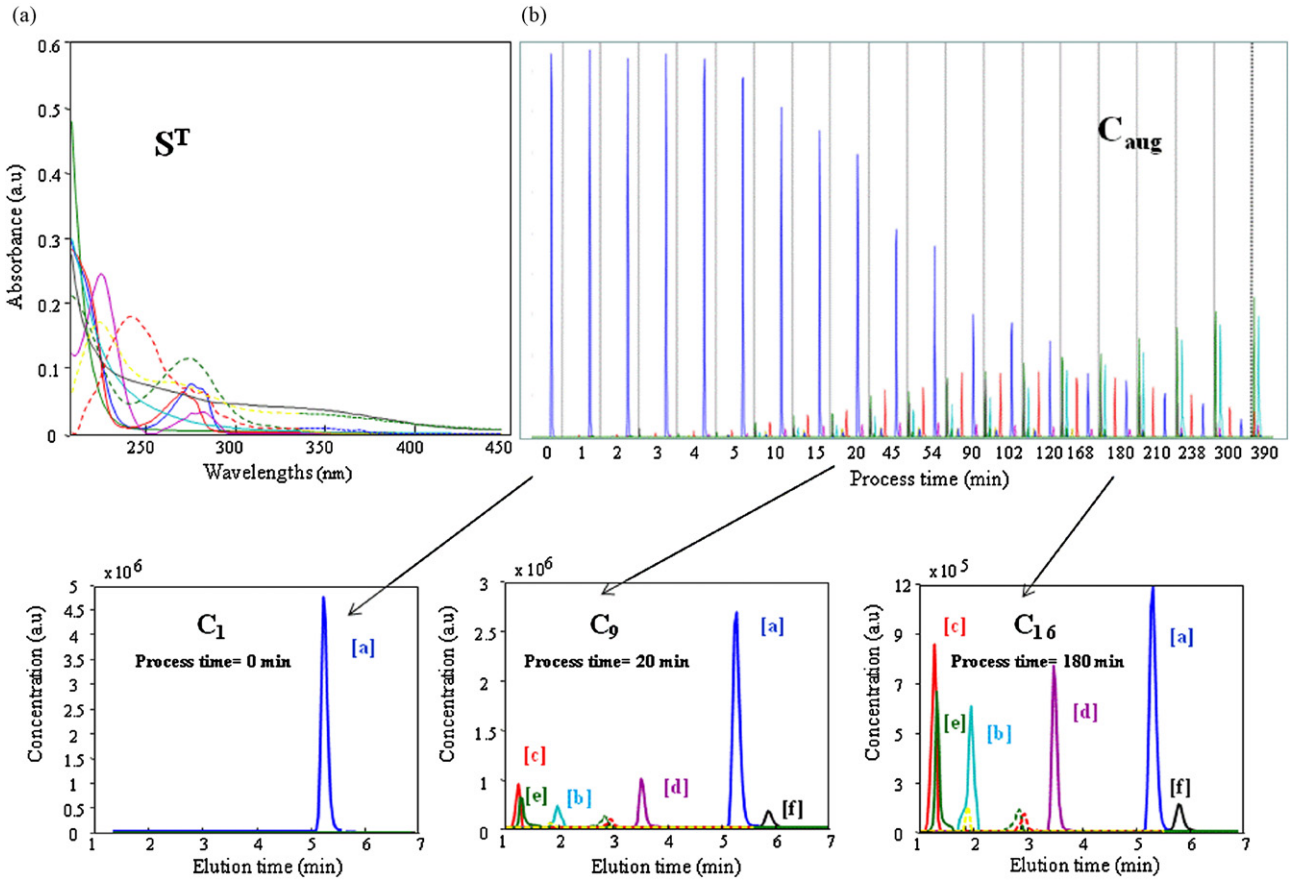

Fig. 4. Simultaneous MCR-ALS analysis of 21 chromatographic runs related to the photodegradation experiment of 2-bromophenol. (a) Pure resolved spectra (matrix $\mathbf{S^T}$) and (b) pure elution profiles related to submatrices of $\mathbf{C_{aug}}$. Bottom plots correspond to zoomed elution profiles related to the extracts collected at process time 0, 20 and 180 min.

by classical UV–vis spectroscopic monitoring, e.g., with spectra collected as a function of time, as could be observed in previous works [27,28]. The complexity of these systems also justifies the different time windows selected to achieve a complete resolution of the data, shown in Table 2. In some analyses, an additional background contribution was needed (particularly in MS data of highly brominated compounds) to improve the resolution results.

Another trend in Table 2 is the lower variance explained and the lower number of resolved components obtained from the analyses of MS data when compared with the DAD results. This can be attributed to two different reasons: the high noise level of MS chromatograms that turned into a lower explained variance and made infeasible the detection of some minor components and the fact that homolog compounds present identical pure MS spectra and, therefore, are identified as a single component with a single spectrum and a multimodal peak. Hence, in many instances, the pure spectra obtained from MS data resolution should be attributed to mixtures of compounds rather than to a single specific species. Furthermore, some arbitrary run-to-run variations of MS intensity data were encountered, which hindered deriving kinetic profiles from the evolution of the peak area of the resolved compounds as a function of process time. And, therefore, the use of the MS results was preferred to be only restricted in the identification of photoproducts. All these differences among DAD and MS results have prevented the simultaneous analysis of DAD and MS fused data, performed in previous works [40]. Thus, DAD results have been considered to offer a good picture of the kinetic evolution of the process because the higher capability of differentiation among single species (particularly, homologs and minor compounds), whereas MS results have been specifically focused on the identification of photoproducts because of the easy interpretation and rich structural information of MS features.

4.1. Photodegradation of monobromophenols

To illustrate the kind of results obtained, analyses of DAD and MS data from the photodegradation experiment of 2-bromophenol will be explained in detail. Twenty-one extracts from light incubations at different process times (from 0 to 390 min) were selected in order to achieve a complete description of the photochemical degradation process.

Fig. 4a and b shows the resolved augmented concentration profiles ($\mathbf{C_{aug}}$) and the related UV–vis pure spectra ($\mathbf{S^T}$) for 2-bromophenol degradation, respectively. Resolution of nine species was achieved with a satisfactory explained variance ($r^2 = 98.6\%$). The inclusion of a different number of species gave lower explained variance or unreliable spectra.

As can be seen, $\mathbf{C_{aug}}$ (Fig. 4b) contains the resolved elution profiles of 21 chromatographic runs corresponding to the extracts collected at the different process times from 0 to 390 min. Fig. 4 also shows zoomed resolved submatrices of $\mathbf{C_{aug}}$ related to the extracts collected at 0, 20 and 180 process time. The zoomed figures allow seeing the MCR-ALS power to resolve very overlapped and minor species. Moreover, it is also remarkable that some of the photoproducts investigated in this work had very similar UV–vis-spectra and, hence, the differences in the elution behavior were crucial to facilitate the distinction of the species involved in the photodegradation process.

Fig. 5 shows the plot of the evolution of the area of the resolved peaks (derived from $\mathbf{C_{aug}}$, see Fig. 1b and data treatment section)

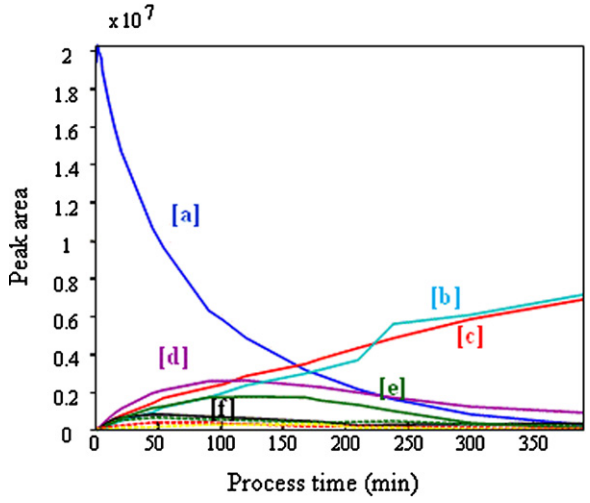

Fig. 5. Evolution of the area of the resolved peaks as a function of process time in the 2-bromophenol photodegradation experiment.

as a function of process time. From this plot, it can be observed the presence of intermediates (labelled [d], [e] and [f]) and end products of photodegradation (labelled [b] and [c]). Similar kinetic evolutions among these products ([d], [e] and [f] and [b] and [c]) are also observed. From the shape of these kinetic profiles, a reaction mechanism based on a sequence of parallel or second- or higher-order reactions is clearly more suitable than a kinetic model based on first-order consecutive reactions.

Once seen the large similarity among the shape of the resolved pure spectra and the similar shape of many kinetic profiles, it is more understandable why the classical UV–vis spectroscopic monitoring would not be adequate for a comprehensive description of the bromophenol photodegradation process (rank-deficiency phenomena would surely be encountered) [41,42]. These phenomena would have translated in chemical terms into the impossibility to distinguish among certain compounds based on their spectral shapes and would have probably mistaken the now more clear complex reaction mechanism (parallel or high-order reaction scheme) for a series of first-order consecutive reactions.

As mentioned before, while the analysis of DAD data allows the resolution of very minor species, homolog species and, hence, provides a global picture of the kinetic evolution of the process, analysis of MS data is needed for the identification of photodegradation products because of the interpretative power of interpretation of MS features.

Fig. 6 shows the MS pure spectra obtained from the resolution of the multiset MS chromatographic data set and their correspondence with the photodegradation products resolved from DAD data (Fig. 5). As stated before, a lower number of resolved components in the analysis of MS data were obtained since, in this case, very minor compounds were not detected with our MS detection system and congeners appear often as single compounds with a multimodal elution profile. For identification, it should be taken into account that the deprotonated molecular ion $(M-H)^-$ of the parental compound and the photodegradation products were obtained due to the fact that ionization source (APCI) was used in negative mode. Based on the molecular weight obtained and on the retention times available for parental compounds, the chemical structures in Fig. 5 were proposed. As it can be seen, the bromine atom of 2-bromophenol (structure [a]) under light irradiation was transferred from the 2-position to the 4-position (structure [f], see retention time of 4-bromophenol), which is in agreement with the result reported by Akai et al. [21]. The typical isotope ratio of $[Br^-]$ and the molecular weight obtained from the MS spectra [c] and [e] suggest

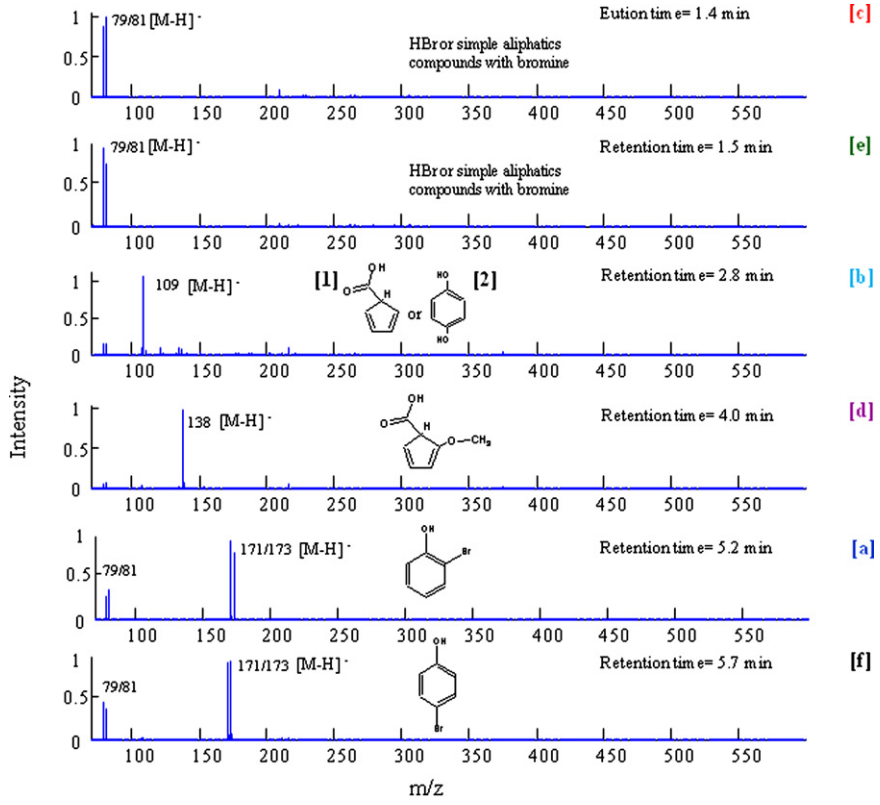

Fig. 6. MS pure spectra and related proposed chemical structures achieved from the MCR-ALS analysis of LC–MS runs obtained during the 2-bromophenol degradation. Compound labels are as in Fig. 5.

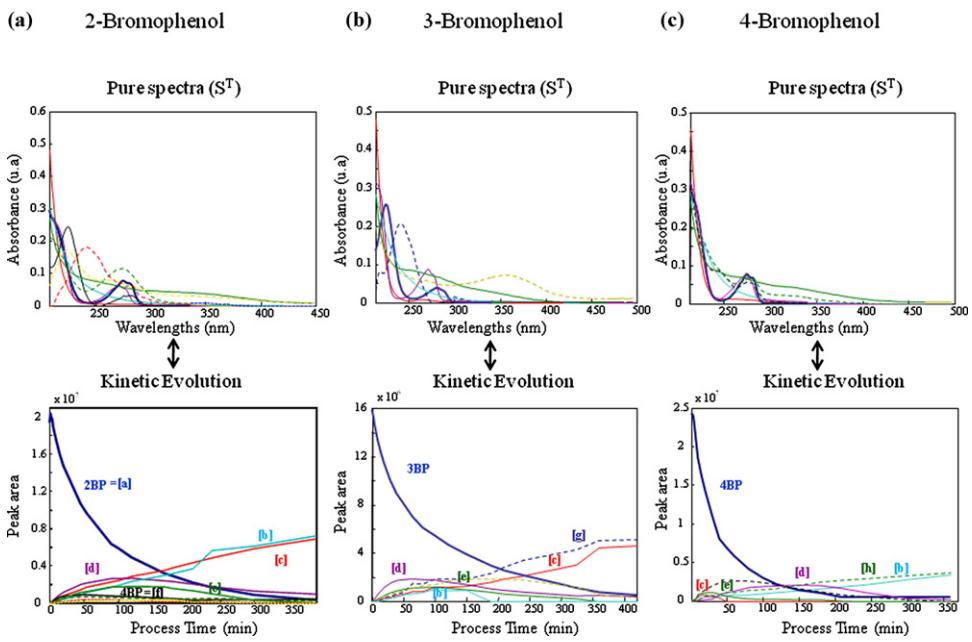

Fig. 7. Evolution of the area of the resolved peaks as a function of process time and related resolved pure spectra ($\mathbf{S^T}$) for the degradation of (a) 2-bromophenol, (b) 3-bromophenol and (c) 4-bromophenol. Compound labels are as in Figs. 5 and 6.

the formation of HBr and simple aliphatic compounds with bromine among the breakdown products, which is in agreement with the results obtained by Joscheck et al. [22] and Lipcynskakochany et al. [26] Moreover, in conformity with these previous works, dihydroxybenzene (structure [b1]) could also be a photodegradation product. Finally, as reported in the photodegradation studies of their homologs, the chlorophenols [19], cyclopentadienic acid (structure [b2]) and methoxy cyclopentadienic acid (structure [d]) have also been suggested.

Fig. 7a–c shows the evolution of peak areas of the resolved compounds as a function of process time and their related UV–vis pure spectra ($\mathbf{S^T}$) for 2-bromophenol, 3-bromophenol and 4-bromophenol, respectively. Thick lines correspond to parental compounds, solid lines are related to common species to all degradation processes and dashed lines are attributed to specific species for each particular bromophenol. Two intermediates, methoxy cyclopentadienic acid ([d]) and HBr or simple aliphatic compounds with bromine ([e]) were common in the three photodegradation experiments. The end products, dihydroxybenzene ([b1]) or cyclopentadienic acid ([b2]) and HBr or simple aliphatic compounds with bromine ([c]) were also common in 2BP and 4BP and 2BP and 3BP photodegradation experiments, respectively. However, the end products [b] and [c] of 2BP photodegradation experiment acted as intermediates in 4BP and 3BP photodegradation experiments, respectively. From the UV–vis pure spectra and the retention times encountered, it is important to note that only the ortho-position of bromine in 2BP tends to promote isomerization process, confirming again the structure of 4BP ([f]) in Fig. 6. Finally, [g] and [h] are unidentified photoproducts of 3BP and 4BP, respectively.

4.2. Photodegradation process of bromophenols with higher degree of bromination

This section describes the results of the analyses of the photodegradation experiments of bromophenols with higher degree of bromination. Once known the methodology needed to obtain the relevant information for photodegradation processes (explained in detail for 2-bromophenol) the presented results will focus on the evolution of the area of the resolved peaks as a function of process time, which provides the kinetic information, and on the identification of the modeled species by MS (the elution profiles and related pure spectra from the resolution results of the multiset chromatographic structures for highly brominated compounds are available on request).

Fig. 8 shows the kinetic evolution of the parental compound and photoproducts for 2,4-dibromophenol (8a), 2,4,6-tribromophenol (8b) and pentabromophenol (8c) degradation processes. The subplots in 8a, b and c refer to the different time windows analyzed (see Fig. 2) for a better visualization.

In Fig. 8, the groups of resolved species that seem to have a similar kinetic evolution have been colored and labeled in the same way. So, now, every capital letter designs a group of compounds with similar kinetic behavior instead of a single species. As in monobromophenol photodegradation experiments, complex kinetic mechanisms based on parallel or high-order reactions could be suggested for the photodegradation of bromophenols with higher degree of bromination. No more mechanistic detail can be given for these systems, since it is virtually impossible to unequivocally find the real reaction scheme among the huge number of potential combinations of parallel and high-order reactions that could be postulated for photodegradations involving such a number of photodegradation products.

It is interesting to note that, in all the photodegradations studied, the sequence of elution is generally inverse to the sequence of the emergence of compounds in the kinetic process. Thus, end products tend to show up in the earliest time window and the slight time differences in the emergence of groups of intermediates show the same chronological trend. This tendency would be consistent with the gradual debromination of these compounds under the action of light. Knowing that homolog groups of bromophenols appear in the same time window owing to their similar elution behavior and having as a reference the retention times available for parental compounds (see Fig. 2), time windows from 1.1 to 6.2 min can be associated to monobromophenol congeners and related photoproducts, time windows from 6.3 to 20.9 min can be related to dibromophenols, tribromophenols and other photoproducts, and time windows from 21.8 to 33.4 min would enclose

Table 3
Chromatographic (retention times) and structural (relevant *m*/*z*) information for photoproducts and parental compounds detected during the bromophenol photodegradation processes. The possible identity and presence in the different degradation processes is detailed for each detect compound.

Retention time		*m*/*z*	Possible compound	Parental compound	Identification in kinetic plots[+]
Time window 1.1–6.2 min	1.3–1.6	79/81	HBr, aliphatic compounds with bromine	2BP, 3BP, 4BP, 24DBP, 246TBP, PBP	[c]$^{\perp}$, [c]$^{\perp}$, [c]$^{\perp}$, [A]*, [A]*, [A]*
	1.5–1.8	79/81	HBr, aliphatic compounds with bromine	2BP, 3BP, 4BP, 24DBP, 246TBP, PBP	[e] $^{\perp}$, [e] $^{\perp}$, [e] $^{\perp}$, [A]*, [A]*, [A]*
	2.8–3.0	109	Dihydroxybenzene, cyclopentadienic acid	2BP, 3BP, 4BP	[b] $^{\perp}$, [b] $^{\perp}$, [b] $^{\perp}$
	2.6–2.8	79/81	HBr, aliphatic compounds with bromine	PBP	[B]*
	2.6–2.8	79/81 135/137	Aliphatic compounds with bromine	24DBP	[B]*
	3.5–3.6	138	Methoxycyclopentadienic acid	2BP, 3BP, 4BP, 24DBP,	[d] $^{\perp}$, [d] $^{\perp}$, [d] $^{\perp}$, [B]*
	3.7–3.8	79/81 265/267/269	Dibromodihydroxybenzene	PBP	[B]*
	4.0–4.2	79/81 189/191	Monobromodihydroxyhexatriene	PBP	[B]*
	5.0–5.5	79/81 171/173	2BP	2BP, 24DBP, 246TBP	[a] $^{\perp}$, [B]*, [B]*
	5.6–5.7	79/81 171/173	3BP	3BP, PBP	3BP$^{\perp}$, [B]*
	5.6–5.8	79/81 171/173	4BP	2BP, 4BP, 24DBP, 246TBP, PBP	[f] $^{\perp}$, 4BP$^{\perp}$, [B]*, [B]*, [B]*
Time window 6.3–20.9 min	6.3–6.6	79/81 343/345/347/349	Tribromodihydroxybenzene	PBP	[D]*
	7.2–7.6	79/81 279/281/283	Dibromohydroxybenzenedione	PBP	[D]*
	7.8–8.0	79/81 249/251/253	Dibromophenol	246TBP; PBP	[C]*, [C]*
	8.2–8.8	79/81 279/281/283	Dibromohydroxybenzenedione	PBP	[D]*
	8.8–9.2	79/81 249/251/253	Dibromophenol	PBP	[C]*
	9.0–9.4	79/81 420/422/424/426/428	Tetrabromohydroxybenzenone	PBP	[C]*
	9.3–10	79/81 249/251/253	24DBP	24DBP, 246TBP, PBP	[C] = 24DBP*, [C]*, [D]*
	12.2–12.6	79/81 279/281/283	Dibromohydroxiybenzenone	PBP	[C]*
	12.2–12.8	79/81 420/422/424/426/428	Tetrabromohydroxybenzenone	PBP	[D]*
	13.8–14.2	79/81 357/359/361/363	Tribromohydroxybenzenone	PBP	[C]*
	14.0–14.8	79/81 327/329/331/333	Tribromophenol	PBP	[D]*
	17.0–18.0	79/81 327/329/331/333	Tribromophenol	PBP	[D]*
	17.7–18.7	79/81 327/329/331/333	Tribromophenol	PBP	[D]*
	18.5–19.7	79/81 327/329/331/333	246TBP	246TBP, PBP	[D]* = 246BP, [D]*
Time window 21.8–33.4 min	23.0–24.0	79/81 435/437/439/441/443	Tetrabromomethoxyphenol	PBP	[E]*
	26.5–27.5	79/81 405/407/409/411/413	Tetrabromophenol	PBP	[E]*
	28.0–29.0	79/81 405/407/409/411/413	Tetrabromophenol	PBP	[E]*
	28.5–29.0	79/81 405/407/409/411/413	Tetrabromophenol	PBP	[E]*
Time window 38.5–48.5 min	42–44	79/81 483/485/487/489/491/493	PBP	PBP	[F]*

[+]The sequence in "Identification in kinetic plots" match with the sequence in "Parental compound", $^{\perp}$ Fig. 7, *Fig. 8

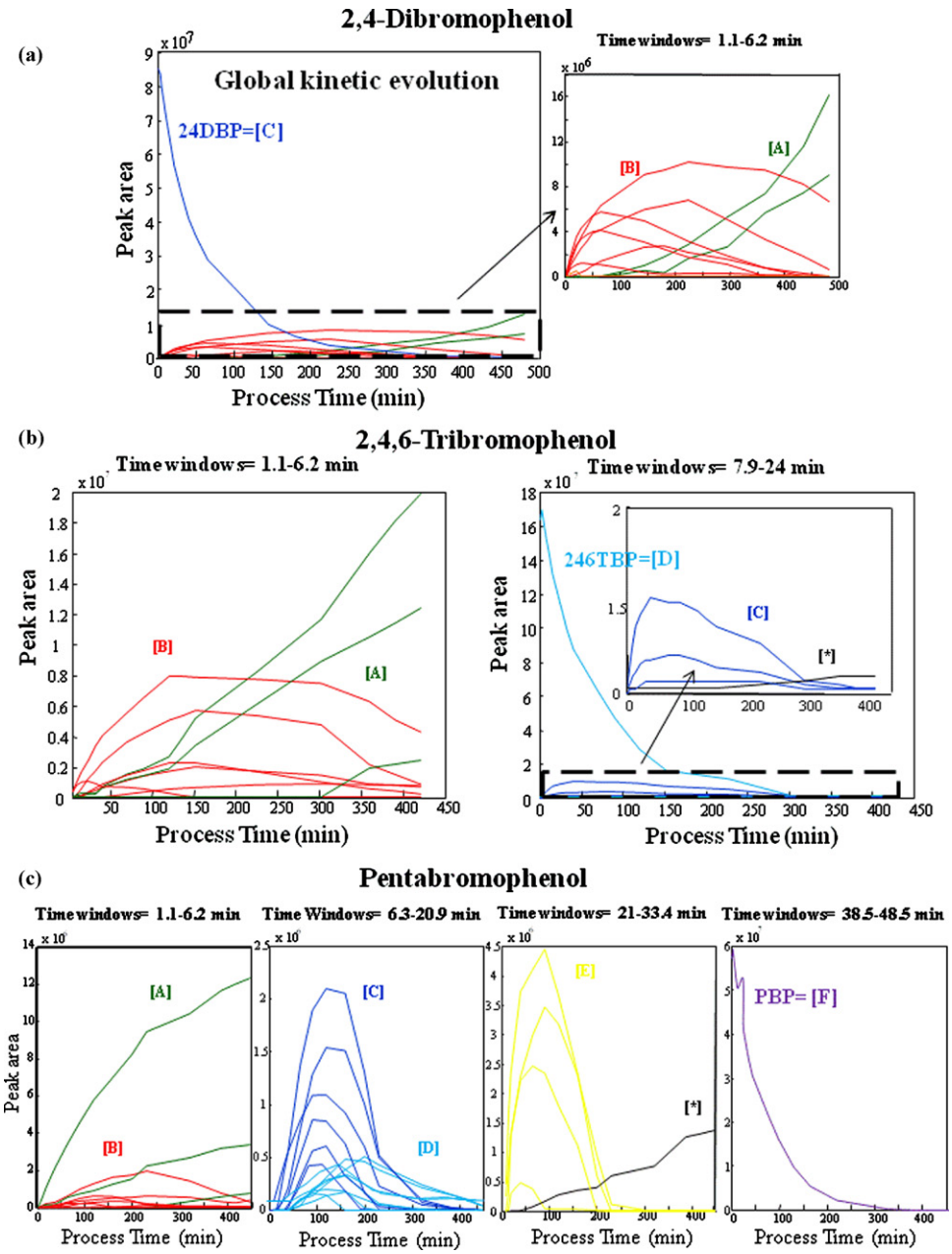

Fig. 8. Evolution of the area of the resolved peaks as a function of process time for the degradation of (a) 2,4-dibromophenol, (b) 2,4,6-tribromophenol and (c) pentabromophenol. Capital letters design groups of compounds with similar kinetic evolution. In general, the sequence [A], [B], [C], [D], [E] and [F] reflects increasing degree of bromination in the related compound class. * are unidentified photoproducts. (The readers should refer to the on-line version to visualize the colors in this figure.)

tetrabromophenols. Therefore, in general, the sequence [A], [B], [C], [D], [E] and [F] in Fig. 8 should be attributed to compounds with an increasing degree of bromination.

To have a more complete interpretation of the formed photoproducts, we investigated the MS resolved spectra for these processes. The information of the photoproducts obtained from the bromophenol experiments is summarized in Table 3, where the identity, the photodegradation origin and the kinetic behavior of more than 30 photoproducts is collected. Photoproducts have been characterized by looking at the features in their mass spectra and at their retention times. In this sense, since the retention times for the parental compounds were available, some of the homologs could be unambiguously identified. In all highly brominated photodegradation experiments, many generated photoproducts were identified as less brominated bromophenols. Thus, reductive debromination by successive losses of bromine atoms is confirmed as the main photodegradation pathway of bromophenols. Besides, other results obtained suggest that substitution of a bromine atom by a hydroxyl groups is also one of the major pathways in the photodegradation process, in agreement with photodegradation mechanisms of chlorophenols [18–20]. Indeed, many compounds with one or more hydroxyl groups can be found in the time windows related to tribrominated and lowly brominated compounds. Due to the limited selectivity of our MS detection system and to the lack of available standards for the large number of potential products formed, it was possible to distinguish between homolog classes (different number of bromine atoms, presence and number of hydroxyl group. . .), but it was not possible to identify within a same class the substitution pattern of the bromine atoms or other functional groups.

After detailing the identity, kinetic evolution and main photodegradation pathways for all bromophenols, a quantitative comparison of the results obtained for the decay of the parental

Table 4
Photolysis decay rate of parental bromophenols.

Bromophenols	K_1 ($\times 10^2$) (min^{-1})
2BP	1.18 (4)[a]
3BP	1.14 (6)
4BP	2.2 (2)
24DBP	1.56 (5)
246TBP	1.67 (4)
PBP	1.8 (2)

[a] Values in parenthesis are the errors related to the estimation of the photolysis decay rates.

compound in the photodegradation experiments of the isomers has been carried out.

Based on the assumption that the photolysis decay of the parental compound follows a pseudo first-order model, the general kinetic equation:

$$[A] = [A]_0 e^{-k_1 t} \quad (6)$$

where k_1 is the rate constant of the photodegradation decay and $[A]$ is the concentration of the parental bromophenol, is fitted to the evolution of the peak area of the compound of interest as a function of process time. At $t = 0$ (standard first aliquot injected before UV light exposure), the peak area of the bromophenol is taken as $[A]_0$. The non-linear Newton–Gauss–Levenberg/Marquardt (NGL/M) algorithm has been used to perform the fitting and obtain the rate constant and its related error [43,44]. Table 4 shows the values of the photolysis decay obtained for each bromophenol studied.

In agreement with the conclusions of reported studies of their analogues (the chlorophenols) bromine position in bromophenols isomers influences significantly on the kinetics of bromophenols photodegradation [19]. The results showed that heterolytic scission of the C–Br bond in the para-position is favorable in direct photolysis, which is probably a result of a steric effect. This is the reason why the 4-bromophenol decays significantly faster than the rest of bromophenols. As a secondary trend, we can conclude that the photodegradation of higher brominated bromophenols seems to be slightly faster than lower brominated compounds, which is in agreement with the conclusions of photodegradation studies of other BFRs [12,17].

5. Conclusions

The results obtained have shown the complexity of the photodegradation processes of bromophenols and the very similar spectra and kinetic evolution of the products obtained justified the use of HPLC–DAD-MS chromatographic monitoring (with the extra information of the elution direction) instead of classical UV–vis spectroscopic monitoring. Analysis of DAD multiset structures provided a good global kinetic picture of the process, since homolog species and minor compounds could be properly distinguished, whereas analysis of MS multiset structures provided the structural information needed to identify the formed photoproducts.

The kinetic information suggests extremely complex reactional schemes, involving many parallel or high-order reactions. Nevertheless, in highly brominated bromophenols, there seems to be different groups of intermediates that follow a sequential emergence and decay. The interpretation of the MS spectra has shown how reductive debromination by successive losses of bromine atoms and substitution of bromine atoms by hydroxyl groups are the main photodegradation pathways of bromophenols. The decay of the parental compounds shows how the bromine position in the monobromophenol isomers influences significantly the kinetics of photodegradation. Thus, bromine in para-position produces an increase of reaction rate. Moreover, a slight increase of the degradation process was observed as the degree of bromination increased.

The combined mathematical and chromatographic resolution method presented here can be proposed as a general procedure for the study of photodegradation processes of a wide variety of environmental pollutants of interest. The time-windowing strategy, the inclusion of the elution direction as a crucial additional information to differentiate among compounds and the use of MS detection for characterization provides a reliable methodology for process analysis of systems involving a very large number of compounds (more than 30 in the case of pentabromophenol). However, the large amount of compounds and the enormous number of possibilities to set reactional schemes in highly brominated systems prevents the unequivocal choice of one preferred scheme over others. In the case of monobromophenols, where less compounds are involved in the photodegradation process, future works will attempt the analysis of fused chromatographic and classical spectroscopic data by the hybrid hard- and soft-modeling MCR-ALS method, with the aim of setting a detailed reaction scheme and derive the related rate constants, providing in this way a more accurate elucidation of the mechanism of these degradation processes.

Acknowledgements

We acknowledge funding from the Spanish government (grant CTQ2009-11572 and CTM2008-03263/TECNO). The authors of this work belong to the network of recognized research groups by the Catalan government (2009 SGR 45). Sílvia Mas acknowledges a Ph.D. grant UAC 2005-0071 from the Ministry of Education and Science (Associated Unit between University of Barcelona and CSIC).

References

[1] C.A. de Wit, Chemosphere 46 (1991) 583.
[2] G. Söderström, U. Sellström, C.A. de Wit, Environ. Sci. Technol. 38 (2004) 127.
[3] J.M. Norris, J.W. Ehrmantraut, C.L. Gibbons, R.J. Kociba, B.A. Schwetz, J.Q. Rose, C.G. Humiston, G.L. Jewett, B.W. Crummett, P.J. Gehring, J.B. Tirsell, J.S. Brosier, Appl. Polym. Symp. 22 (1973) 195.
[4] I. Watanabe, R. Tatsukawa, Bull. Environ. Contam. Toxicol. 39 (1987) 953.
[5] S. Otha, H. Nishimura, T. Nakao, O. Aozasa, H. Miyata, Organohalogen Compd. 52 (2001) 321.
[6] J. Eriksson, N. Green, G. Marsh, A. Bergman, Environ. Sci. Technol. 38 (2004) 3119.
[7] A. Palm, I.T. Cousins, D. Mackay, Environ. Pollut. 117 (2002) 195.
[8] J. Bezares-Cruz, C.T. Jafvert, I. Hua, Environ. Sci. Technol. 38 (2004) 4149.
[9] L. Sánchez-Prado, M. Lores, M. Llompart, C. García-Jares, J.M. Bayona, R. Cela, J. Chromatogr. A 1124 (2006) 157.
[10] I. Hua, N. Kang, C.T. Jafvert, J.R. Fábrega-Duque, Environ. Toxicol. Chem. 22 (2003) 798.
[11] J. Niu, Z. Shen, Z. Yang, X. Long, G. Yu, Chemosphere 64 (2006) 658.
[12] M. Barcellos da Rosa, H.-U. Krüger, S. Thomas, C. Zetzsch, Fresenius Environ. Bull. 12 (2003) 940.
[13] M.Y. Ahn, T.R. Filley, C.T. Jafvert, L. Nies, I. Hua, J. Bezares-Cruz, Environ. Toxicol. Chem. 40 (2006) 215.
[14] M.Y. Ahn, T.R. Filley, C.T. Jafvert, L. Nies, I. Hua, J. Bezares-Cruz, Chemosphere 64 (2006) 1801.
[15] A. Palm, R. Kopetzky, W. Sossinka, W. Ruck, C. Zetzsch, Organohalogen Compd. 66 (2004) 4105.
[16] J.D. Raff, R.A. Hites, Environ. Toxicol. Chem. 41 (2007) 6725.
[17] J. Eriksson, S. Rahm, N. Green, A. Bergman, E. Jakobsson, Chemosphere 54 (2004) 117.
[18] M. Czaplicka, A. Czaplicki, J. Photochem. Photobiol. A 178 (2006) 90.
[19] H.D. Burrows, L.S. Ernestova, T.J. Kemp, Y.I. Skurlatov, A.P. Purmal, A.N. Yermakov, Prog. React. Kinet. Mech. 23 (1998) 145.
[20] S. Rayne, K. Forest, K.J. Friesen, Environ. Int. 35 (2009) 425.
[21] N. Akai, S. Kudoh, M. Takayanagi, M. Nakata, Chem. Phys. Lett. 363 (2002) 591.
[22] H.I. Joschek, S.I. Miller, J. Am. Chem. Soc. 88 (1966) 3269.
[23] F. Bonnichon, C. Richard, G. Grabner, Chem. Commun. (2001) 73.
[24] G. Guyon, P. Boule, J. Lemaire, Nouv. J. Chim. 8 (1984) 685.
[25] G. Grabner, C. Richard, Hdb. Env. Chem. 2 (2005) 161.
[26] E. Lipczynskakochany, Chemosphere 24 (1992) 911.
[27] S. Mas, A. de Juan, S. Lacorte, R. Tauler, Anal. Chim. Acta 618 (2008) 18.
[28] M. de Luca, S. Mas, G. Ioele, F. Oliverio, G. Ragno, R. Tauler, Int. J. Pharm. 386 (2010) 99.
[29] A. de Juan, M. Maeder, M. Martínez, R. Tauler, Chemom. Intell. Lab. Syst. 54 (2000) 123.

[30] R. Tauler, Chemom. Intell. Lab. Syst. 30 (1995) 133.
[31] R. Tauler, A. Smilde, R. Kowalski, J. Chemom. 9 (1995) 31.
[32] S.D. Brown, R. Tauler, B. Walczak (Eds.), Comprehensive Chemometrics, vol. 2, Elsevier, 2009, pp. 325–344.
[33] S.D. Brown, R. Tauler, B. Walczak (Eds.), Comprehensive Chemometrics, vol. 2, Elsevier, 2009, pp. 473–506.
[34] K. Johnson, A. De Juan, S.C. Rutan, J. Chemom. 13 (1999) 331.
[35] E. Bezemer, S.C. Rutan, Chemom. Intell. Lab. Syst. 60 (2002) 239.
[36] A. De Juan, R. Tauler, J. Chromatogr., A 1158 (2007) 184.
[37] P. Jonsson, A.I. Johansson, J. Gullberg, J. Trygg, A. Jiye, B. Grung, S. Marklund, M. Sjöström, H. Antti, T. Moritz, Anal. Chem. 77 (2005) 5635.
[38] Y. Shen, R. Zhang, R.J. Moore, J. Kim, T.O. Metz, K.K. Hixson, R. Zhao, E.A. Livesay, H.R. Udseth, R.D. Smith, Anal. Chem. 77 (2005) 3090.
[39] J. Jaumot, R. Gargallo, A. de Juan, R. Tauler, Chemom. Intell. Lab. Syst. 76 (2005) 101.
[40] E. Peré-Trepat, R. Tauler, J. Chromatogr., A 1131 (2006) 85.
[41] M. Amrhein, B. Srinivasan, D. Bonvin, M.M. Schumacher, Chemom. Intell. Lab. Syst. 33 (1996) 17.
[42] A. Izquierdo-Ridorsa, J. Saurina, S. Hernández-Cassou, R. Tauler, Chemom. Intell. Lab. Syst. 38 (1997) 183.
[43] M. Maeder, A.D. Zuberbühler, Anal. Chem. 62 (1990) 2220.
[44] G. Puxty, M. Maeder, K. Hungerbühler, Chemom. Intell. Lab. Syst. 81 (2006) 149.